Integrating Metabolic and Anatomical Imaging: Insights from FDG PET-CT in Brain Malignancies

1 Fatema Tuz Zohra, 1Priyanka Podder, 2Rayhan Alam, 2Md. Abul Hasnat, 3Tanvir Ahmed Biman, 4 Tania Sultana, 5 Md. Selim Reza

[1]Senior Medical Officer, Institute of Nuclear Medical Physics (INMP), AERE
[2]Senior Scientific Officer, [3]Principal Scientific Officer, INMP
[4]Senior Medical Officer, Institute of Nuclear Medicine and Allied Sciences (INMAS), Dhaka.
[5]Director and Chief Scientific Officer, INMP

Correspondence Address: Dr. Fatema Tuz Zohra, Senior Medical Officer, INMP, AERE, Savar, Dhaka- 1349 Email: shetu0000@gmail.com

ABSTRACT

Objective: To evaluate the metabolic and anatomical characteristics of brain malignancies using ^{18}F-FDG PET-CT, with emphasis on diagnostic and clinical relevance.

Methods: A retrospective analysis of 2,879 FDG PET-CT scans performed between January 2019 and December 2023 at the Institute of Nuclear Medical Physics (INMP), Savar. Parameters assessed included lesion metabolic activity (SUVmax), anatomical localization, CT appearance, and correlation with histopathological diagnosis.

Results: Seventeen patients were identified with malignant brain lesions. Among them, three were primary gliomas, two were primary CNS lymphomas, and twelve were metastatic lesions—originating from breast (n = 4), lung (n = 3), carcinoma of unknown origin (n = 3), prostate (n = 1), and tongue (n = 1). High-grade gliomas exhibited markedly elevated SUVmax values.

Conclusion: FDG PET-CT delineated tumor margins and multifocal disease accurately, complementing MRI by providing essential metabolic data for staging and treatment planning. Further prospective studies are recommended to define its prognostic utility.

Keywords: FDG PET-CT, Brain Tumor, Glucose Metabolism, Metastatic Lesions, Neuro-Oncology, CNS Imaging

Bangladesh J. Nucl. Med. Vol. 29 No. 1 January 2026
DOI: https://doi.org/10.3329/bjnm.v29i1.89282

INTRODUCTION

The application of ^{18}F fluorodeoxyglucose (^{18}F FDG) in PET-CT has transformed oncologic imaging by providing a noninvasive measure of tissue glucose metabolism (1). Malignant cells demonstrate increased glycolytic activity even under aerobic conditions, a phenomenon known as the “Warburg effect” (2). This characteristic allows FDG PET-CT to detect metabolic alterations before structural changes become apparent.

However, the brain’s intrinsic metabolic activity presents a unique diagnostic challenge. Approximately 20% of the body’s glucose is consumed by the brain, resulting in naturally high FDG uptake in the grey matter (3). Consequently, delineating malignant lesions from normal cortex can be difficult, particularly for low-grade tumors with low metabolic rates (4). Despite these limitations, FDG PET-CT has proven useful in differentiating high-grade gliomas, CNS lymphomas, and metastatic lesions from benign or necrotic tissue (5).

The integration of metabolic and anatomical imaging has advanced neuro-oncologic evaluation significantly. PET-CT not only assists in tumor grading but also in distinguishing recurrent tumor from post-radiation necrosis, assessing treatment response, and detecting systemic metastases (6). Several studies have demonstrated that FDG uptake patterns strongly correlate with tumor aggressiveness and survival outcomes (7, 8). Furthermore, the fusion of PET with MRI or CT enhances lesion localization and image interpretation, thereby improving overall diagnostic accuracy (9).

Despite its growing global use, data from Bangladesh on PET-CT-based brain malignancy assessment are limited. Despite its increasing global utilization, there remains a paucity of data from Bangladesh regarding PET-CT–based evaluation of brain malignancies. This retrospective study from INMP aims to provide institutional experience correlating metabolic and anatomical features in brain malignancies, highlighting the clinical relevance of FDG PET-CT in routine neuro-oncology practice.

PATIENTS AND METHODS

A retrospective observational study was conducted using the INMP PET-CT database comprising 2,879 patient cases from January 2019 to December 2023. Inclusion criteria covered all patients referred for PET-CT with confirmed or suspected CNS malignancy. Demographic data, lesion type, site, metabolic uptake, and CT morphology were analyzed.

Patients fasted for at least six to eight hours prior to imaging, followed by intravenous administration of 18F FDG. Scanning commenced 60 minutes post-injection using a Philips 128-slice Ingenuity TF scanner. Images were reconstructed using iterative algorithms, and standardized uptake values (SUVmax) were measured for all lesions.

RESULTS

Out of a total of 2,879 patients who underwent FDG PET-CT scan (Table 1), 17 cases (0.6%) were diagnosed with brain malignancy. Among these patients, 9 (52.9%) were male and 8 (47.1%) were female. The mean age of the patients was 52 ± 14 years, indicating that most of the cases occurred in middle-aged to older adults.

Table 1. Demographic distribution among brain malignancy patients attending Institute of Nuclear Medical Physics

Variable	Frequency (n)	Percentage (%)	
Total Patients		2,879	100.0
Brain Malignancy		17	0.6
Male	9	52.9	
Female	8	47.1	

Among the 17 patients diagnosed with brain malignancies, the lesions were classified into primary brain tumors (n = 5; 29.4%) and metastatic brain lesions (n = 12; 70.6%) (Table 2). Among the primary brain malignancies, high-grade gliomas- including glioblastoma multiforme (GBM) and astrocytoma- were most common (3 cases; 17.6%). Within the metastatic group, the most frequent sources of brain metastasis were breast carcinoma (4 cases; 23.5%) and lung carcinoma (3 cases; 17.6%).

Table 2. Distribution of Brain Lesion Types and Origins

Lesion Category	Specific Type / Primary Origin	Frequency (n)	Percentage (%)
Primary Brain Malignancies (n=5)	High-grade Glioma (GBM & Astrocytoma)	3	17.6
	Primary CNS Lymphoma	2	11.8
Metastatic Brain Lesions (n=12)	Breast Carcinoma	4	23.5
	Lung Carcinoma	3	17.6
	Carcinoma of Unknown Origin	3	17.6
	Prostate Carcinoma	1	5.9
	Tongue Carcinoma	1	5.9
Total		**17**	**100.0**

A comparative analysis of metabolic and imaging characteristics between primary brain malignancies (n = 5) and metastatic brain lesions (n = 12) demonstrated distinct patterns on PET-CT (Table 3). The primary brain tumors exhibited higher metabolic activity with SUV_{max} values ranging from 9.8 to 18.2 (mean ± SD = 13.7 ± 3.1). In contrast, metastatic brain lesions showed a lower mean SUV_{max} (5.2–14.5; mean ± SD = 9.1 ± 2.8) on PET imaging.

Table 2. Distribution of Brain Lesion Types and Origins

Parameters	Primary Brain Malignancies (n = 5)	Metastatic Brain Lesions (n = 12)
Common Histologic Types	High-grade Glioma (n = 3); Primary CNS Lymphoma (n= 2)	Breast Carcinoma (n = 4); Lung Carcinoma (n = 3); Carcinoma of Unknown Origin (n = 3); Prostate Carcinoma (n = 1); Tongue Carcinoma (n = 1)
SUV_{max} Range (mean ± SD)	9.8 – 18.2 (13.7 ± 3.1)	5.2 – 14.5 (9.1 ± 2.8)
Lesion Multiplicity	Usually, solitary	Frequently multiple (2–6 lesions)

On non-contrast CT evaluation, the density characteristics of brain lesions varied among the 17 diagnosed cases illustrated in Figure 1. A total of 8 cases (47.1%) appeared hyperdense. Six cases (35.3%) were identified as hypodense. The remaining 3 cases (17.6%) were isodense.

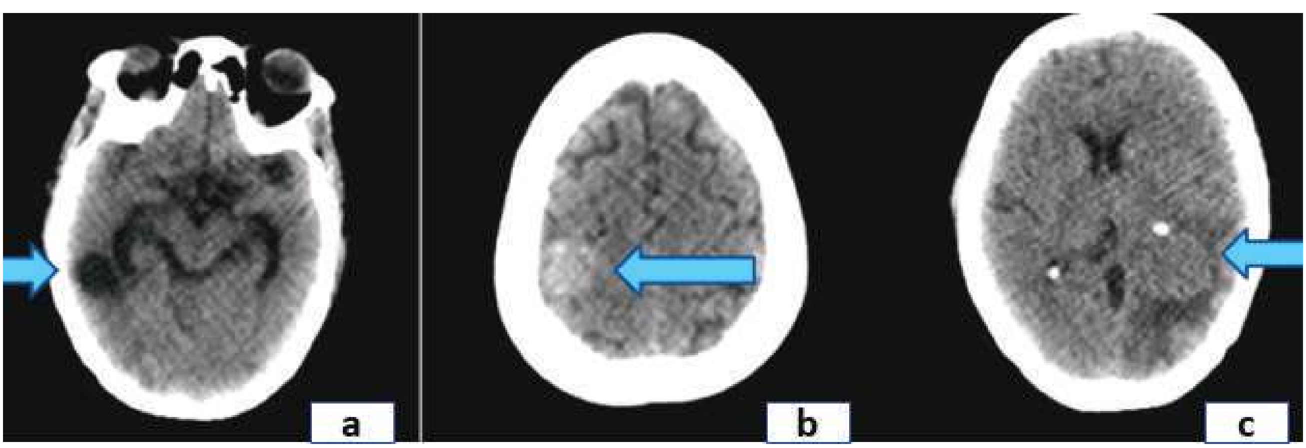

Figure 1. Pattern of anatomical findings in axial CT images. Hypodense lesion in right temporal lobe (a, blue arrow), Hyperdense lesion in right frontal lobe (b, blue arrow), Isodense lesion on left parietal lobe (c, blue arrow).

On FDG PET imaging, metabolic activity among brain lesions varied widely depicted in Figure 2. Out of the 17 cases, 8 lesions (47.1%) demonstrated hypermetabolic activity with SUV_{max} values ranging from 7.5 to 29.0, indicating high glucose uptake consistent with aggressive or high-grade tumors. Hypometabolic uptake was observed in 6 lesions (35.3%), showing SUV_{max} between 5.2 and 9.1, typically corresponding to low-grade with reduced metabolic function. In contrast, 3 lesions (17.6%) were classified as isometabolic, with SUV_{max} values between 6.2 and 8.2.

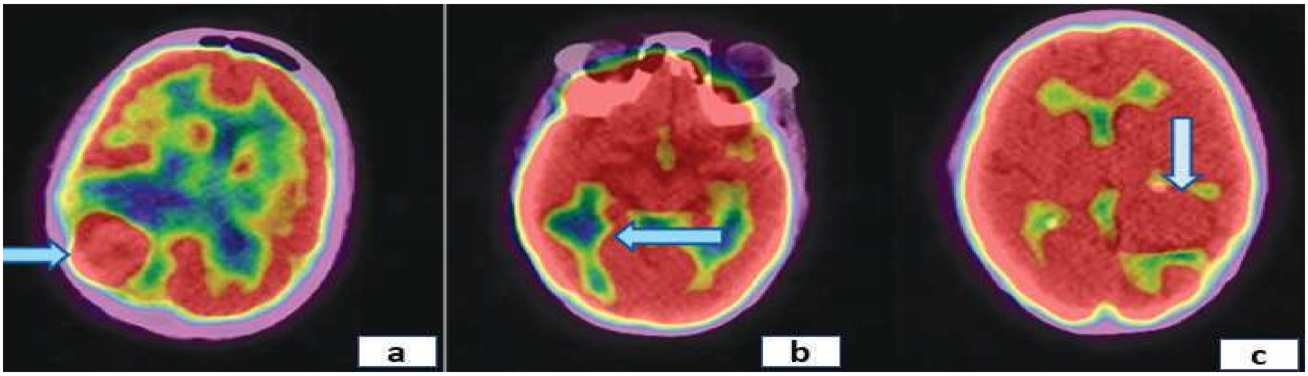

Figure 2. Metabolic pattern on PET axial images. Hypermetabolic lesion with SUV_{max} 29.0 in the right parietal lobe (a, blue arrow); Hypometabolic lesion with SUV_{max} 5.2 in the right temporal lobe (b, blue arrow); Isometabolic lesion with SUV_{max} 8.2 in the left parietal lobe (c, blue arrow).

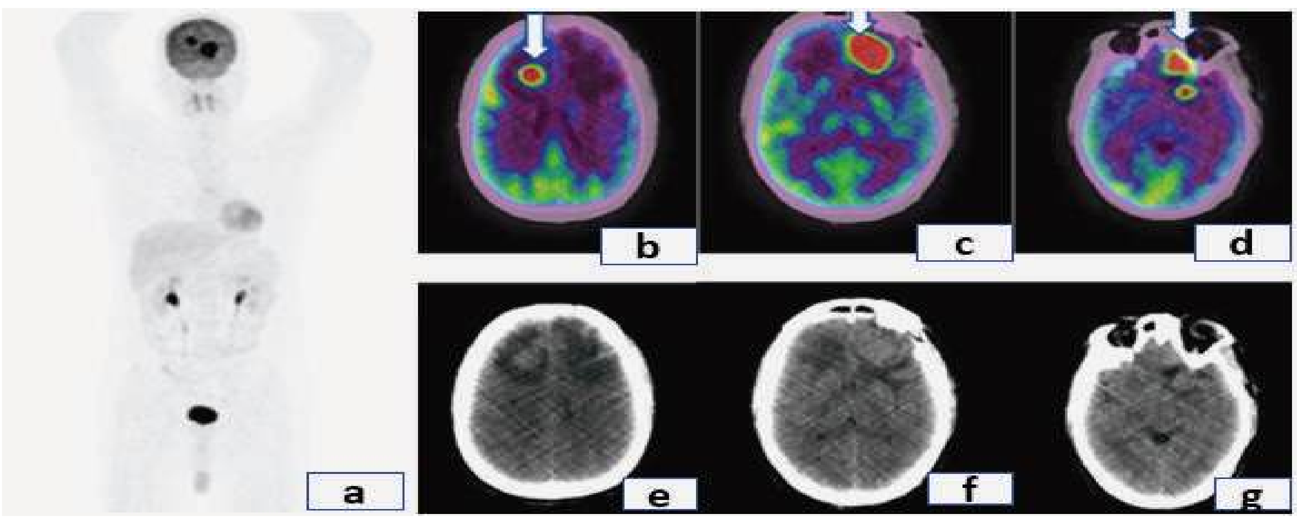

Figure 3: A 32-year-old male patient with CNS non-Hodgkin lymphoma. The MIP image (a) shows a focal FDG-avid mass involving both frontal lobes, with a maximum SUV of approximately 29.0. Corresponding axial CT images (b–d) and fused PET-CT images (e–g) demonstrate an iso- to hyperdense lesion (white arrow) with surrounding perilesional hypodense edema.

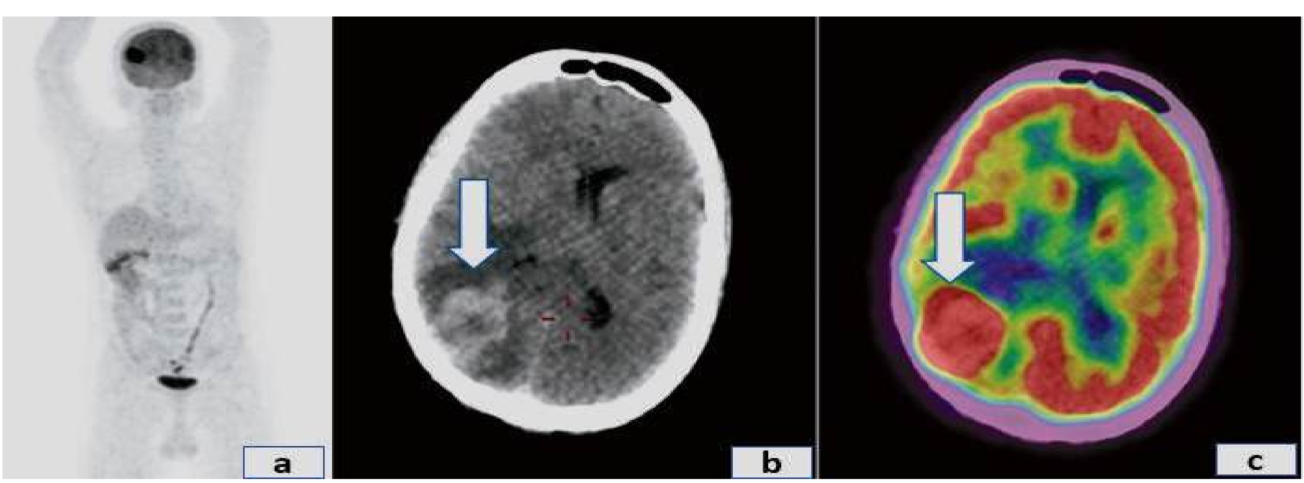

Figure 4: A 42-year-old male with CNS glioma. The MIP image (a) and fused PET-CT image (c) show a focal FDG-avid mass in the right occipital lobe, with a maximum SUV of 25.7 (white arrow). The corresponding axial CT image (b) demonstrates a hyperdense lesion with surrounding perilesional hypodense edema (white arrow).

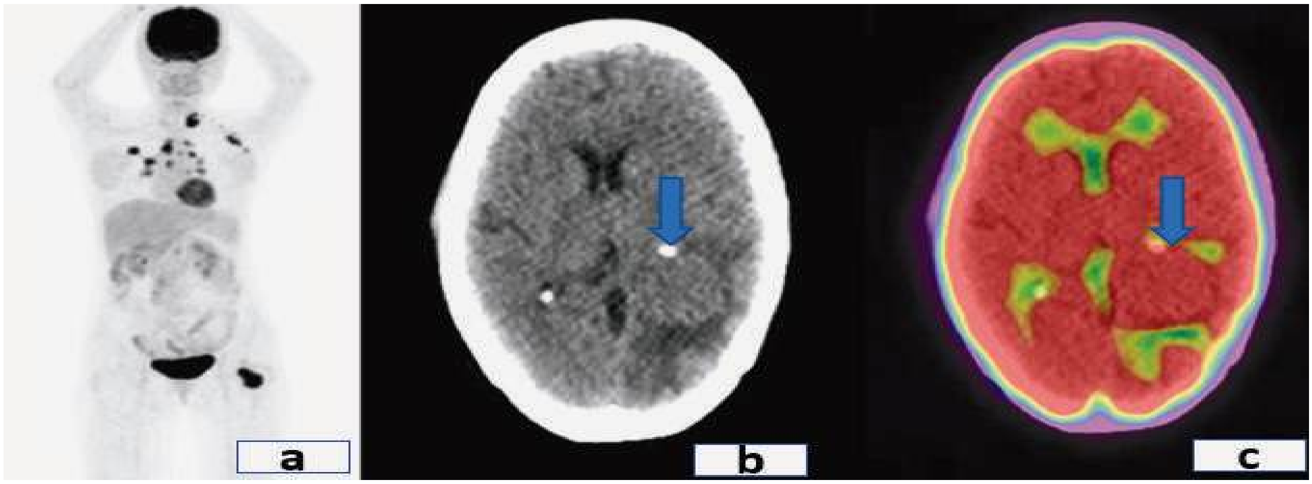

Figure 5: A 55-year-old female with adenocarcinoma of the right lung and skeletal and supraclavicular lymph node metastases. The MIP image (a) and fused axial PET-CT (c, blue arrow) show an intensely hypermetabolic soft-tissue mass in the left parietal region, with a maximum SUV of 16. Corresponding axial CT (b) and fused PET-CT (c) images demonstrate an isodense lesion (b, blue arrow) with surrounding edema and associated shift of the left lateral ventricle.

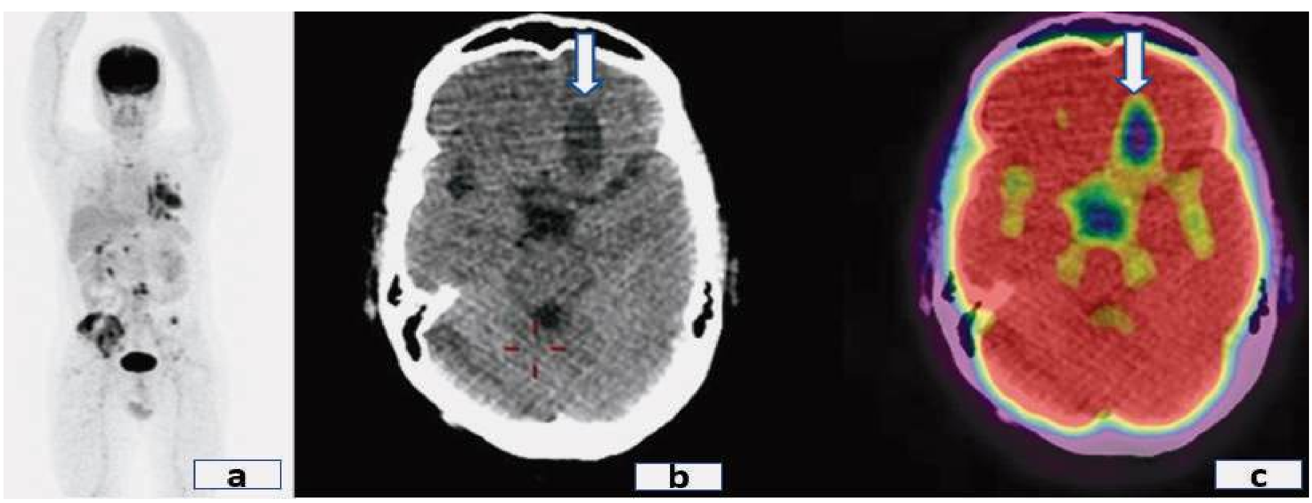

Figure 6: A 58-year-old male with squamous cell carcinoma of the left lung and skeletal and brain metastases. The MIP image (a) with the corresponding axial CT (b, white arrow) and fused PET-CT (c, white arrow) images demonstrating a hypodense, hypometabolic lesion in the left frontal lobe (white arrow).

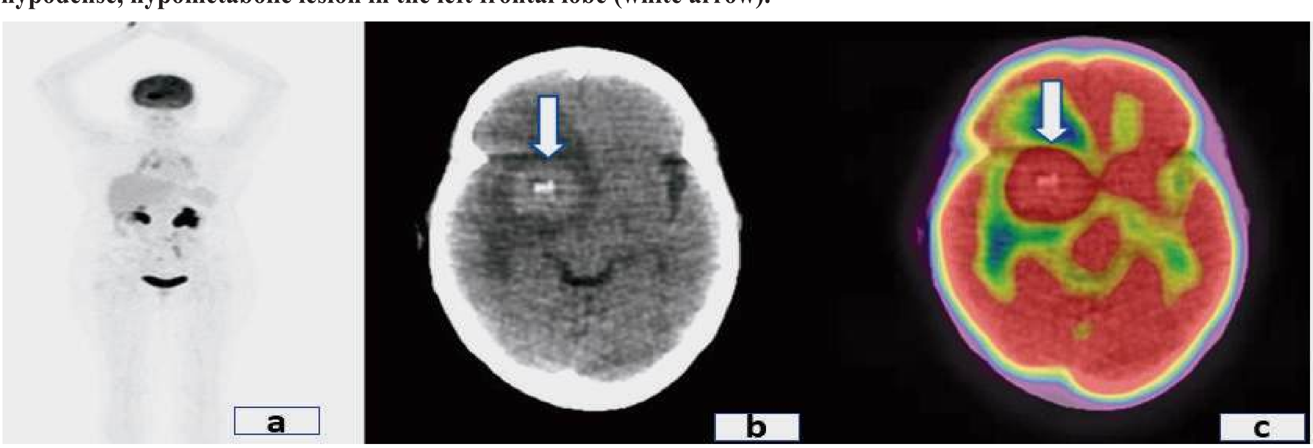

Figure 7: A 47-year-old female with carcinoma of the left breast and skeletal and brain metastases. The MIP image (a) with the corresponding axial CT (b, white arrow) and fused PET-CT (c, white arrow) images demonstrating a large iso- to hypodense right frontal lobe lesion with mass effect and hypermetabolism (SUVmax 12.7) (white arrow).

DISCUSSION

The findings of this retrospective analysis highlight the significant clinical value of FDG PET-CT in evaluating CNS malignancies in a Bangladeshi tertiary nuclear medicine setting. Among 2,879 PET-CT scans, only 17 cases (0.6%) showed malignant brain lesions, reaffirming that CNS involvement is relatively uncommon in patients undergoing whole-body PET-CT surveillance, a trend also reported in earlier studies of oncologic PET cohorts (4).

A major observation in the present study is the predominance of metastatic brain lesions (70.6%) over primary brain tumors (29.4%). This aligns with global epidemiology indicating that intracranial metastases outnumber primary CNS neoplasms in PET-CT datasets, particularly among patients with breast and lung cancers, both of which were leading sources of metastasis in our cohort (12). The relatively higher representation of breast carcinoma (23.5%) and lung carcinoma (17.6%) is consistent with international metastatic patterns previously highlighted in nuclear medicine literature (5).

The study demonstrates clear distinctions in metabolic behavior between primary and metastatic lesions. High-grade gliomas and CNS lymphomas showed markedly elevated SUVmax values (mean 13.7 ± 3.1), reflecting their aggressive glycolytic phenotype. This finding supports earlier reports showing sensitivities between 86% and 95% for high-grade gliomas and up to 90% for CNS lymphomas on FDG PET-CT, attributed to their robust glucose metabolism (11). The highest SUVmax (~29.0) recorded in a CNS lymphoma case is fully aligned with previous evidence describing lymphomas as among the most FDG-avid intracranial malignancies (10).

In contrast, metastatic lesions demonstrated variable metabolic activity depending on histology and SUVmax values (mean 9.1 ± 2.8), reflecting an observation also noted in earlier comparative studies (12, 13). Lung metastases generally showed intense uptake, while breast and prostate metastases often presented with moderate or mixed metabolic patterns, consistent with prior findings on systemic metastatic behavior (8).

Non-contrast CT findings varied widely, with nearly half of the lesions appearing hyperdense. This reinforces the importance of metabolic correlation, as FDG uptake adds functional specificity to anatomical information. Earlier publications have emphasized that PET-CT markedly improves diagnostic confidence when CT density alone is inconclusive, particularly in differentiating necrotic, cystic, or hemorrhagic lesions (4, 14).

The study corroborates the established role of FDG PET-CT in neuro-oncology, especially for high-grade lesions where metabolic activity is high. PET-CT is known to assist in delineating tumor margins, particularly in hypermetabolic gliomas and lymphomas (7); identifying multifocal metastatic disease, which was common in our series; assessing treatment response, where reductions in SUVmax correlate with improved survival (13); and differentiating recurrence from post-radiation necrosis, an area where PET-CT often provides greater clarity than MRI alone (14).

Recent literature also supports the complementary use of amino acid tracers (e.g., 11C-methionine, 18F-FET) for low-grade or recurrent tumors to overcome the inherent limitation of physiologic cortical FDG uptake (15). While amino acid PET is not currently available in Bangladesh, the present study confirms that FDG PET-CT remains a highly informative modality when combined with anatomical CT and clinical context.

Published data in Bangladesh on PET-CT evaluation of brain tumors remain limited. This study provides one of the largest institutional datasets from the country, demonstrating characteristic metabolic and anatomical trends in both primary and metastatic brain malignancies. Our findings closely parallel SUVmax ranges and imaging behavior described in international series, supporting the robustness and reliability of PET-CT interpretation in the local clinical environment (6, 10).

CONCLUSION

FDG PET-CT proved highly useful in characterizing both primary and metastatic brain malignancies, with primary high-grade gliomas and CNS lymphomas showing markedly higher metabolic activity than metastatic lesions. The integration of metabolic and anatomical data improved diagnostic accuracy, lesion localization, and assessment of multifocal disease.

Despite physiologic brain uptake, PET-CT effectively complemented MRI and provided clinically relevant information for staging and treatment planning. These findings support the continued use of FDG PET-CT as a valuable tool in the routine neuro-oncologic workflow in Bangladesh.

REFERENCES

1. AC11084030 A, editor. Standard operating procedures for PET/CT: a practical approach for use in adult oncology. Internat. Atomic Energy Agency; 2013.
2. Warburg O. On the origin of cancer cells. Science. 1956 Feb 24;123(3191):309-14.
3. Brown RK, Bohnen NI, Wong KK, Minoshima S, Frey KA. Brain PET in suspected dementia: patterns of altered FDG metabolism. Radiographics. 2014 May;34(3):684-701.
4. Fink JR, Muzi M, Peck M, Krohn KA. Continuing education: Multi-modality brain tumor imaging–MRI, PET, and PET/MRI. Journal of nuclear medicine: official publication, Society of Nuclear Medicine. 2015 Aug 20;56(10):1554.
5. Riahi F, Kiani P, Golabbakhsh A, Khanezarrin M, Abbaspour M, Tabatabaei SA, Fesharaki S, Tooyserkani SH, Bakhshi R, Azizollahi S, Mohammadi H. Comparison of PET/CT and PET/MRI in central nervous system tumors, a narrative review. International journal of physiology, Chiavazza C, Pellerino A, Ferrio F, Cistaro A, Soffietti R, Rudà R. Primary CNS Lymphomas: Challenges in Diagnosis and Monitoring. Biomed Res Int. 2018 Jun 21;2018:3606970. doi: 10.1155/2018/3606970. PMID: 30035121; PMCID: PMC6033255.
6. Coenen HH, Elsinga PH, Iwata R, Kilbourn MR, Pillai MR, Rajan MG, Wagner Jr HN, Zaknun JJ. Fluorine-18 radiopharmaceuticals beyond [18F] FDG for use in oncology and neurosciences. Nuclear medicine and biology. 2010 Oct 1;37(7):727-40.
7. Hatzoglou V, Ulaner GA, Zhang Z, Beal K, Holodny AI, Young RJ. Comparison of the effectiveness of MRI perfusion and fluorine-18 FDG PET-CT for differentiating radiation injury from viable brain tumor: a preliminary retrospective analysis with pathologic correlation in all patients. Clinical imaging. 2013 May 1;37(3):451-7.
8. Hawkins RA, Hoh C, Glaspy J, Rege S, Choi Y, Phelps ME. Positron emission tomography scanning in cancer. Cancer investigation. 1994 Jan 1;12(1):74-87.
9. Albano D, Bertoli M, Battistotti M, Rodella C, Statuto M, Giubbini R, Bertagna F. Prognostic role of pretreatment 18F-FDG PET/CT in primary brain lymphoma. Annals of nuclear medicine. 2018 Oct;32(8):532-41.
10. Nihashi T, Dahabreh IJ, Terasawa T. PET in the clinical management of glioma: evidence map. American Journal of Roentgenology. 2013 Jun;200(6):W654-60.
11. Fei B, Schuster DM. PET molecular imaging–directed biopsy: a review. American Journal of Roentgenology. 2017 Aug;209(2):255-69.
12. Verger A, Kas A, Darcourt J, Guedj E. PET imaging in neuro-oncology: an update and overview of a rapidly growing area. Cancers. 2022 Feb 22;14(5):1103.
13. Rahman A. Positron-emission tomography (PET) and single-photon-emission computed tomography (SPECT) Diagnosis of Neurological disorders. Bangladesh Journal of Medicine. 2025;36(1):3-14.
14. Albano D, Bosio G, Bertoli M, Giubbini R, Bertagna F. 18F-FDG PET/CT in primary brain lymphoma. Journal of Neuro-Oncology. 2018 Feb;136(3):577-83.
15. Näslund O, Smits A, Förander P, Laesser M, Bartek Jr J, Gempt J, Liljegren A, Daxberg EL, Jakola AS. Amino acid tracers in PET imaging of diffuse low-grade gliomas: a systematic review of preoperative applications. Acta Neurochirurgica. 2018 Jul;160(7):1451-60.